ULTRACOMPACT AND HIGH-GAIN THIN-FILM BULK ACOUSTIC RESONATOR MAGNETOELECTRIC ANTENNA ARRAY

Bin Luo[1], Xianfeng Liang[1], Huaihao Chen[1], Neville Sun[1], Hwaider Lin[2] and Nian X. Sun[1*]*
[1] Northeastern University, Boston, Massachusetts, USA
[2] Winchester Technologies LLC, Burlington, Massachusetts, USA

ABSTRACT

Magnetoelectric (ME) antennas exhibit ultra-compact sizes comparable to acoustic wavelength and enhanced radiation performance on a ground plane compared to conventional electrical antennas, showing great potential in IoT, 5G, and biomedical applications. This study first utilizes parallel and series FBAR ME antenna array topology to achieve a profound gain and radiation efficiency enhancement without degrading impedance matching and quality factor of ME resonators. Notably, 10 dBi gain enhancement is achieved in the 3×3 FBAR ME array by increasing the array element number, realizing a high gain of −17.3 dBi. We also demonstrate ground plane immunity and 3-dB gain enhancement on ground planes with different shapes. The demonstrated FBAR ME antenna arrays are outstanding platform-independent ultra-compact high-gain conformal antenna candidates for wireless communication, wireless power transfer, and portable electronic and biomedical devices.

KEYWORDS

Magnetoelectric (ME) Antennas, Thin-Film Bulk Acoustic resonators (FBAR), Ultrahigh-frequency (UHF) Antenna Arrays, Portable Electronic And Biomedical Devices.

INTRODUCTION

In recent decades, the escalating demand for compact, low-profile, and high-gain antennas has been driven by the proliferation of applications such as Internet-of-Things (IoTs), 5th generation (5G) wireless systems, and implantable medical devices [1-3]. In contrast to conventional electrical antennas typically larger than one-tenth of the electromagnetic wavelength (λ_{EM}), magnetoelectric (ME) antennas operate on electromechanical resonance and exhibit sizes comparable to the acoustic wavelength, which is 5 orders of magnitude smaller than λ_{EM} [4]. Utilizing magnetic currents for radiation, ME antennas display immunity to detuned antenna impedance and enhanced performance on surfaces like metallic planes or the human body [5].

Noteworthy advancements in ultrahigh-frequency (UHF) thin-film bulk acoustic resonator (FBAR) and solid-mounted resonator (SMR) ME antennas have yielded ultra-small designs with 1-2 orders of magnitude miniaturization over state-of-the-art compact antennas [6, 7]. Recent breakthroughs, including self-biased and passive dual-band UHF ME antennas employing three parallel ME resonators, have garnered significant attention in the biomedical community due to their high magnetic field sensitivity and exceptional wireless power transfer efficiency [8].

However, despite the successful demonstration of high-performance single UHF ME antennas and very low-frequency (VLF) ME antenna arrays [9], the experimental implementation of a UHF ME antenna array remains unexplored. Here we present the experimental demonstration of FBAR ME antenna arrays with seven distinct topologies, achieving a remarkable 10 dBi gain enhancement compared to a single ME antenna without degrading impedance matching and quality factor of the ME resonator. Notably, this marks the first demonstration of a UHF FBAR ME antenna array, distinguishing itself from [6-8] in array topology and from [9] in UHF ME antenna array elements. The impedance of the ME antenna array tends to increase with the number of elements in series and decrease with elements in parallel. Leveraging these insights, we propose that augmenting the number of elements in series, incorporating ME resonators with varying anchor widths in parallel, and ensuring impedance alignment at 50 Ω during the resonant frequency yield a compact and energy-efficient FBAR ME antenna array with exceptionally high gain and broad frequency bandwidth. This breakthrough presents compelling opportunities in the realms of multiband or wideband UHF wireless communication, wireless power transfer, and portable electronic and biomedical devices.

Furthermore, the ground plane immunity of FBAR ME antennas is also demonstrated experimentally, leading to 3-dB gain enhancement mounted on a ground plane and strong adaptability/flexibility to ground planes with different shapes. These advantageous characteristics make FBAR ME antennas excellent for portable implantable biomedical devices and other application scenarios involving ground planes.

MICRO-NANO FABRICATION OF FBAR ME ANTENNA ARRAY

We experimentally demonstrated the 7 ME antenna arrays with different numbers of serial and parallel ME resonator disks. The array topology includes 1×1, 1×2, 1×3, 2×2, 3×2, 2×3 and 3×3. The optical images of 1×1, 1×3, 2×2, and 3×3 FBAR ME antenna arrays are shown in Figure 1. The schematic and scanning electron microscopy (SEM) image of a 1×1 ME antenna is shown in Figure

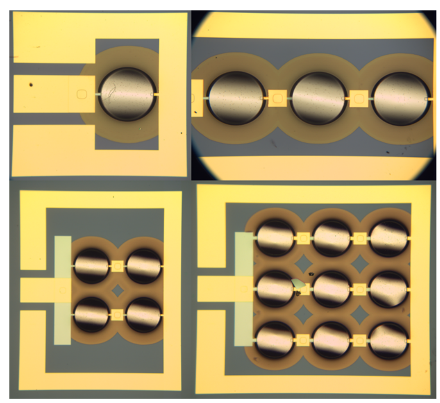

Figure 1: Optical images of 4 released FBAR ME antenna arrays with different number of ME disks.

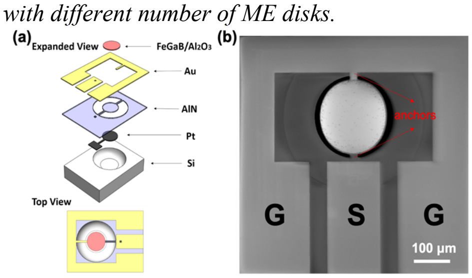

Figure 2: (a) Schematics of FBAR ME antenna. (b) Scanning Electron Microscopy (SEM) image of FBAR ME antenna with ground-signal-ground (GSG) pads.

2. Starting from a high-resistivity (> 10000 Ω·cm) Si wafer, we formed bottom electrodes by sputter-depositing and lift-off patterning a 50-nm-thick Pt film. Subsequently, a 500 nm AlN film was sputter-deposited, and vias were etched through H_3PO_4. The AlN resonant nano-plate was defined through Inductively Coupled Plasma (ICP) Cl_2 etching. A 100 nm thick gold (Au) film was evaporated and lifted off to create the top electrode. A 500 nm thick FeGaB/Al_2O_3 multilayer was then deposited by magnetron sputtering, followed by lift-off patterning. Ultimately, the structure was released through XeF_2 isotropic etching of the silicon substrate to ensure a strong thickness mode acoustic resonance. The resonator was patterned to be a 200 µm disk and the geometry of the Au top electrode was designed for GSG probe feeding and S parameter measurements. The detailed fabrication process can be found in [6].

GROUND PLANE IMMUNITY DEMONSTRATION

To investigate the resilience to ground plane effects of strain-mediated thin-film bulk acoustic resonator (FBAR) magnetoelectric (ME) antennas, we assessed their antenna gains in the presence of variously sized metallic substrates. Our experimental setup involved positioning five square copper ground planes (GPs) beneath an FBAR ME antenna chip. These GPs varied in size, with side lengths increasing from 1 to 7.5 cm as the GP label number progressed from 1 to 5. The antenna, characterized by a resonance frequency of 1.953 GHz and a bandwidth of 8.4 MHz, was examined for gain fluctuations attributable to these underlying platforms.

To ensure precise gain measurements, particularly considering the diminutive scale of ME antennas, a 2 cm × 2 cm plastic substrate matching the thickness of the GPs was used as a reference. Notably, as illustrated in Figure 3, the antenna's input impedance remained constant across different GPs, while its gain showed a significant increase of 3.5 dB. This increase is remarkable given the minimal impact of GP size on the gain enhancement, likely due to the antenna's compact size with a diameter of merely 200 µm.

This gain improvement of 3 dB is a direct consequence of the FeGaB/SiO2 magnetic stack's role in enhancing our ME antenna's performance. We attribute the demonstrated ground plane immunity and gain enhancement to the generation of in-phase magnetic image currents, contrasting with the out-of-phase imaging currents from conductive electric currents typically employed in conventional antennas. The magnetic current dynamics within the stack stem from oscillations in magnetization and corresponding flux dynamics, driven by magnetoelectric coupling and the electromechanical resonance of the piezoelectric layer.

Our findings underscore the substantial promise of FBAR ME antennas, utilizing ME coupling in magnetostrictive/piezoelectric composites, for applications in portable and implantable biomedical devices, among other scenarios where ground planes are involved.

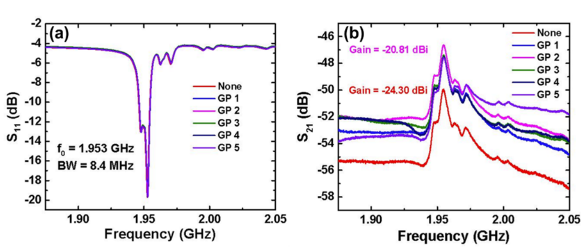

Figure 3: Demonstration of ground plane immunity and 3-dB gain enhancement of FBAR ME antenna. (a) Return loss curves (S_{11}) of ME FBAR of resonance frequency (f_0) of 1.953 GHz and bandwidth (BW) of 8.4 MHz mounted on different sizes of ground planes. (b) Transmission curves (S_{21}) of ME FBAR antenna mounted on different ground planes. GP 1: 1 cm× 1 cm. GP 2: 2 cm× 2 cm. GP 3: 3 cm× 3 cm. GP 4: 4 cm× 4 cm. GP 5: 7.5 cm× 7.5 cm. None: 2 cm× 2 cm plastic substrate.

GAIN AND RADIATION PATTERN

The investigation into the performance of seven magnetoelectric (ME) antenna arrays, each configured with varying serial and parallel arrangements of ME resonator disks, has yielded significant insights, as detailed in Figure 4. All arrays operate within a narrow frequency range of 2.51 to 2.53 GHz, demonstrating effective control over the thickness vibration modes of individual ME resonator disks. With the incremental addition of resonator disks, there is a corresponding increase in antenna gain, reaching a peak of −17.3 dBi in the 3×3 FBAR ME array configuration, as depicted in Figure 4(g)-(h). The nonlinear relationship between the number of array elements and antenna gain is likely due to alterations in input impedance and resultant impedance mismatches as more resonator disks are incorporated. The gain enhancement and considerable changes in the array's impedance are supported by the increases in the S_{21} parameter and significant shifts in the S_{11} parameter relative to the number of elements, respectively.

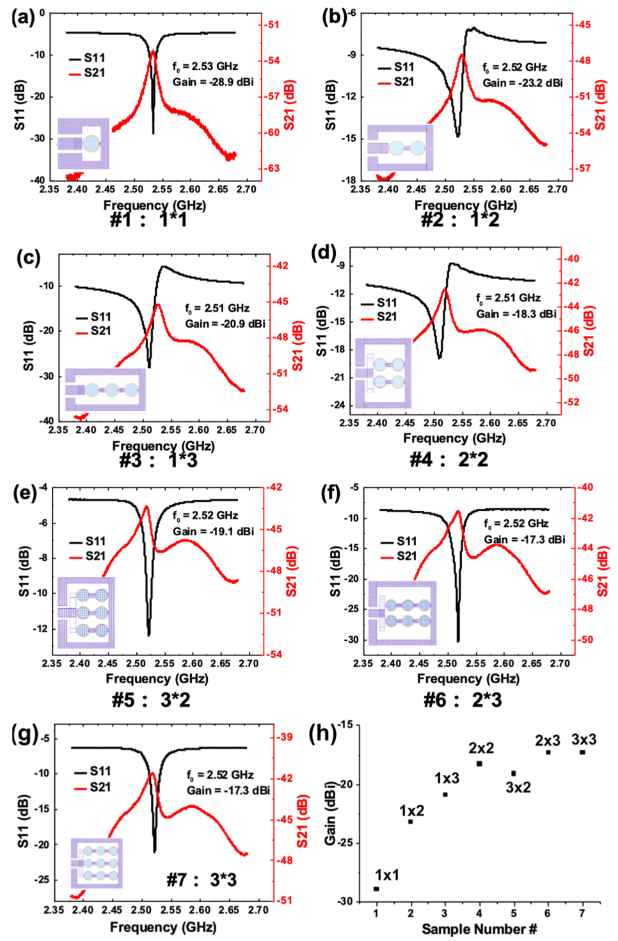

Figure 4: S parameters and gain of FBAR ME antenna arrays. (a) #1: 1 × 1. (b) #2: 1 × 2. (c) #3: 1 × 3. (d) #4: 2 × 2. (e) #5: 3× 2. (f) #6: 2 × 3. (g) #7: 3×3. (h) Gain enhancement of FBAR ME antenna array. The insets show the mask designs.

The radiation patterns of both the 3×3 ME and dipole ME antenna arrays [10] are presented in Figure 5. The ME antenna gain

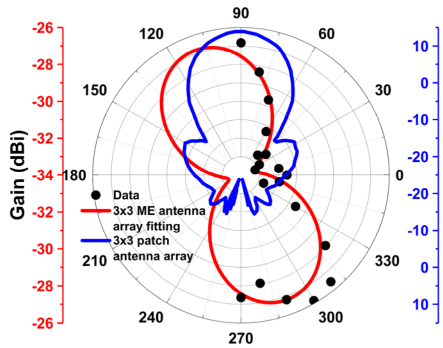

Figure 5: Comparison of radiation pattern of 3×3 ME antenna array and 3×3 patch antenna array [10]. The measured data (black dots) are fitted to the ME antenna array radiation pattern (red curve). The radiation pattern of the ME antenna array is similar to a single ME antenna [6], where the gain is enhanced but the directivity does not change. However, the directivity changes for the 3×3 patch antenna array compared with the single patch antenna.

measured at various angles aligns well with the theoretical magnetic dipole radiation pattern [6]. Unlike conventional electrical antenna arrays, ME antenna arrays enhance radiation efficiency without notably affecting directivity. They maintain the characteristics of a magnetic dipole source owing to their overall dimensions significantly smaller than one-quarter of the electromagnetic wavelength. The FBAR ME antenna array particularly benefits from consistent impedance matching via n×n topology, given each element is tuned to optimal MBVD parameters and 50 ohms input impedance for good impedance matching. This characteristic allows for the assembly of a compact, high-performance antenna array with good impedance matching. Besides, the aforementioned ground plane immunity and 3-dB gain enhancement when mounted on a ground plane make the array particularly suitable for wearable and biomedical applications.

Further insights are provided in Figure 6(a)-(c), which summarizes the impedance, resistance, and reactance of the seven arrays. Resistance predominantly determines the impedance's magnitude and shape, with minimal impact from reactance. The impedance trends indicate an increase in the number of elements aligned serially along the anchor length, as shown in the group of 1×1(#1), 1×2(#2), and the group of 1×3(#3) 3×2(#5) and 3×3(#7). In addition, a decrease with elements added in parallel across the anchor width was shown in the group of 1×3(#3), 2×3(#6), and 3×3(#7) as well as the group of 1×2(#2), 2×2(#4) and 3×2(#5). This analysis suggests that optimizing the number of elements in series, varying anchor widths in parallel configurations, and ensuring impedance matching at the resonant frequency can yield a compact, energy-efficient FBAR ME antenna array. This approach holds significant potential for enhancing gain and broadening frequency bandwidth, paving the way for advancements in multiband or wideband UHF wireless communication, wireless power transfer, and portable electronic and biomedical devices.

EQUIVALENT CIRCUIT ANALYSIS

The FBAR ME antenna array is conceptualized as networks of MBVD circuits of ME resonators arranged in series and parallel, as illustrated in Figure 6(g). The equivalent MBVD model of the ME antenna array is detailed in Figure 6(h). Variations in model parameters across different array sizes and configurations are graphically represented in Figures 6(d)-(f).

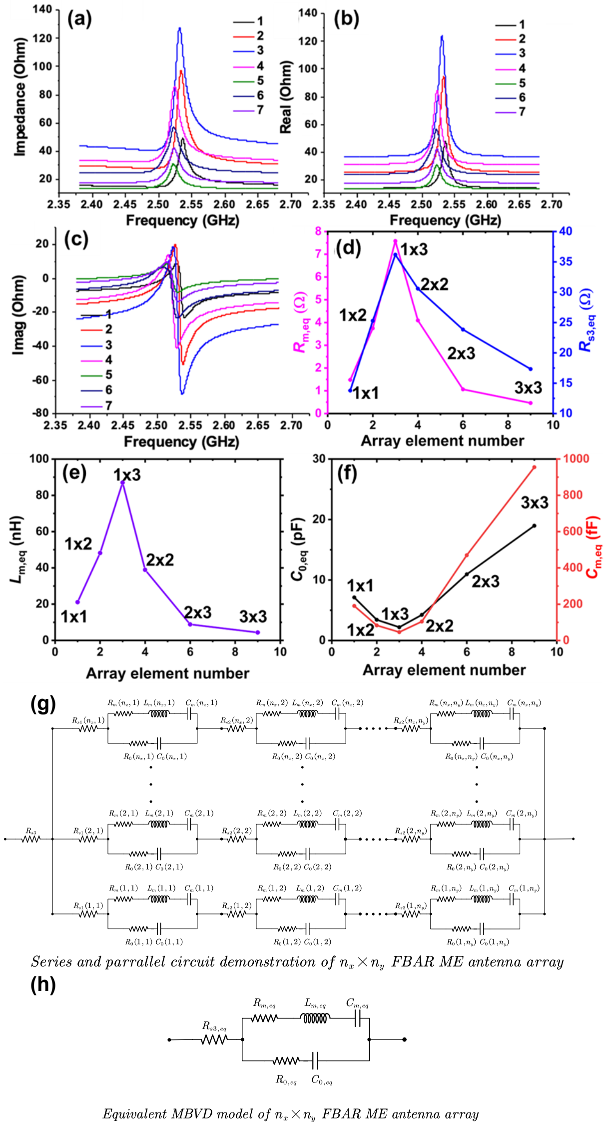

Figure 6: Impedance and equivalent MBVD model parameters as a function of array element number and array topology (a) Impedance plots of all ME antenna arrays. (b) Real part of impedance plots of all ME antenna arrays. (c) Imaginary part of impedance plots of all ME antenna arrays. (d) Motional resistance $R_{m,eq}$ (acoustic loss) and electrode resistance $R_{s3,eq}$ (electrode parasitic ohmic loss). (e) Motional inductance $L_{m,eq}$. (f) Static plate capacitance $C_{0,eq}$ and motional capacitance $C_{m,eq}$. (g) Series and parallel circuit demonstration of n_x×n_y FBAR ME antenna array (h) Equivalent MBVD model of n_x×n_y FBAR ME antenna array. ME antenna array ID: ***#1:*** *1 × 1.* ***#2:*** *1 × 2.* ***#3:*** *1 × 3.* ***#4:*** *2 × 2.* ***#5:*** *3× 2.* ***#6:*** *2 × 3.* ***#7:*** *3 × 3.*

As the array configuration expands from a 1×1 to a 1×3, there is an observed increase in equivalent mechanical resistance $R_{m,eq}$, electrode resistance $R_{s3,eq}$, and motional inductance $L_{m,eq}$, while static plate capacitance $C_{0,eq}$ and motional capacitance $C_{m,eq}$ tend to decrease. This behavior aligns with the series connection of MBVD circuits. However, when the array size increases beyond four elements, a notable shift occurs: $R_{m,eq}$, $R_{s3,eq}$ and $L_{m,eq}$ decrease, and $C_{0,eq}$ and $C_{m,eq}$ increase. This unexpected trend suggests a deviation from the initial predictions which assume uniform MBVD parameters of ME resonator elements throughout the array. It highlights the need for stringent control in the micro-nano fabrication process to maintain consistent MBVD parameters of ME resonator units within and among arrays, crucial for designing and achieving superior high-gain ME antenna arrays.

To explore the relationship between antenna gain and input impedance, Table 1 presents these metrics as they vary with the number of array elements and array topology. As the element count rises from 1 to 3, the magnitude of the reflection coefficient increases due to a rise in input impedance, leading to suboptimal impedance matching and a consequent decrease in power input for radiation. This reduction slows the enhancement of antenna gain with the array element number. Further increases in array size (from 4 to 6 and then to 9 elements) result in compromised impedance, which negates the gains achieved from increasing the number of elements, ultimately stabilizing the antenna gain at −17.3 dBi. Optimizing the array topology to ensure a 50-ohm input impedance for efficient impedance matching, while also increasing the array element number, is crucial for developing high-performance ME antenna arrays suitable for wireless communication, wireless power transfer, and biomedical applications.

Table 1: Relation among antenna gain, element number, and input impedance for ME antenna arrays

ME antenna array topology	Array element number	Input impedance (ohm) at the highest transmission S_{21}	$\lvert S_{11}\rvert$(dB)	Antenna gain (dBi)
1×1	1	44.48−2.33i	−23.9	−28.9
1×2	2	82.56−11.43i	−11.72	−23.2
1×3	3	110.11−7.43i	−8.45	−20.9
2×2	4	71.98−10.19i	−14.07	−18.3
3×2	6	26.34−8.14i	−9.74	−19.1
2×3	6	51.38−2.88i	−30.03	−17.3
3×3	9	35.93−8.26i	−14.47	−17.3

CONCLUSION

In this study, we experimentally demonstrated FBAR ME antenna arrays with series and parallel topologies and realized significantly enhanced gain and radiation efficiency. The micro-fabricated seven array topologies—1×1, 1×2, 1×3, 2×2, 3×2, 2×3, and 3×3 displayed resonant frequencies between 2.51 and 2.53 GHz, illustrating precise control over the thickness vibration modes of the individual ME resonator disks. A significant 10 dBi gain increase was found in the 3×3 FBAR ME array, which achieved a maximum antenna gain of −17.3 dBi. The relationship between gain enhancement and the number of elements was nonlinear, likely due to the variations in input impedance and subsequent impedance mismatches as more resonator disks were added. Notably, the impedance of the ME antenna array increased with the addition of elements in series and decreased when elements were added in parallel.

Unlike traditional electrical antenna arrays, the ME antenna array enhances radiation efficiency without significantly impacting directivity, owing to its ultra-compact dimensions far smaller than one-quarter of an electromagnetic wavelength. By strategically selecting the number of series and parallel elements and ensuring a 50 Ω impedance at the resonant frequency, the FBAR ME antenna array can achieve exceptionally high gain, superior radiation efficiency, and broad frequency bandwidth. This opens promising avenues for its use in multiband or wideband UHF wireless communication, wireless power transfer, and portable electronic and biomedical devices.

Additionally, the demonstrated ground plane immunity and 3-dB gain enhancement of the FBAR ME antenna mounted on various ground plane shapes establishes it as an excellent choice for a platform-independent, conformal antenna suitable for portable implantable biomedical devices and other applications that require compatibility with diverse ground plane configurations.

ACKNOWLEDGEMENTS

Bin Luo, Xianfeng Liang, and Huaihao Chen contributed equally to this work and are co-first authors. This work is partially supported by the NIH Award UF1NS107694 and by the NSF TANMS ERC Award 1160504.

REFERENCES

[1] L. Lizzi, F. Ferrero, P. Monin, C. Danchesi and S. Boudaud, “Design of miniature antennas for IoT applications”, 2016 IEEE Sixth International Conference on Communications and Electronics (ICCE), Ha-Long (2016), pp. 234-237.

[2] W. Hong, Z. Jiang and C. Yu *et al.*, “Multibeam Antenna Technologies for 5G Wireless Communications,” *IEEE Transactions on Antennas and Propagation,* 65, 12 (2017).

[3] A. Kiourti, and K. Nikita, “A Review of Implantable Patch Antennas for Biomedical Telemetry: Challenges and Solutions”, *IEEE Antennas and Propagation Magazine,* 54, 3 (2012).

[4] H. H. Chen, X. F. Liang and C. Z. Dong *et al.*, “Ultra-compact mechanical antennas”, *Applied Physics Letters,* 117, 17 (2020).

[5] X. F. Liang, H. H. Chen and Z. Q. Hu *et al.*, “Experimental Demonstration of Ground Plane Immunity for Magnetoelectric Antennas”, 2022 IEEE MTT-S International Microwave Workshop Series on Advanced Materials and Processes for RF and THz Applications, IMWS-AMP, Guangzhou (2022), pp. 1-3.

[6] T. X. Nan, H. Lin and Y. Gao *et al.*, “Acoustically actuated ultra-compact NEMS magnetoelectric antennas”, *Nature Communications,* 8, 1 (2017).

[7] X. Liang, H. Chen and N. Sun *et al.*, “Mechanically Driven Solidly Mounted Resonator-Based Nanoelectromechanical Systems Magnetoelectric Antennas”, *Advanced Engineering Materials*, 25, 21 (2023).

[8] M. Zaeimbashi, M. Nasrollahpour and A. Khalifa *et al.*, “Ultra-compact dual-band smart NEMS magnetoelectric antennas for simultaneous wireless energy harvesting and magnetic field sensing”, *Nature Communications,* 12, 1 (2021).

[9] C. Z. Dong, Y. F. He and M. G. Jeong *et al.*, “Acoustically Actuated Magnetoelectric Antenna Arrays for VLF Radiation Enhancement”, 2022 IEEE International Symposium on Phased Array Systems & Technology (PAST), Waltham (2022), pp. 1-4.

[10] R. Vilaltella Esteve, *Master Thesis*, Universität Stuttgart, 2013.

CONTACT

*Bin Luo, tel: +1-617-309-6845; luo.bin1@northeastern.edu
*Nian X. Sun, tel: +1-781-775-8878; n.sun@northeastern.edu